Title
Effects of Cyclic Temperature Variations on Thermal Response of an Energy Pile under a Residential Building

Journal
Journal of Geotechnical and Geoenvironmental Engineering, 145(10)

ISSN
1090-0241

Authors
Faizal, Mohammed
Bouazza, Abdelmalek
McCartney, John S
et al.

Publication Date
2019-10-01

DOI
10.1061/(asce)gt.1943-5606.0002147

Peer reviewed

Effects of cyclic temperature variations on the thermal response of an energy pile under a residential building

by

Mohammed Faizal

PhD Student, Monash University, Department of Civil Engineering, 23 College Walk, Clayton, Vic. 3800, Australia. Telephone: +61 3 9905 8901; Email: mohammed.faizal@monash.edu

*** Abdelmalek Bouazza (Corresponding Author)**

Professor, Monash University, Department of Civil Engineering, 23 College Walk, Clayton, Vic. 3800, Australia. Telephone: +61 3 9905 4956; Email: malek.bouazza@monash.edu

John S. McCartney

Professor and Department Chair, University of California San Diego, Department of Structural Engineering, 9500 Gilman Drive, SME 442J, La Jolla, CA 92093-0085, USA, Telephone: +1 858 534 9630; Email: mccartney@ucsd.edu

Chris Haberfield

Principal, Golder Associates Pty. Ltd., Building 7, Botanicca Corporate Park, 570–588 Swan St., Richmond, Vic. 3121, Australia. Telephone: +61 3 8862 3586; Email: chaberfield@golder.com.au

Abstract

The effects of daily cyclic temperature variations on the thermal response of an energy pile built under a six-level residential building are examined. The axial and radial thermal strains along the length of the pile followed stable, linear reversible paths during daily active heating and cooling cycles corresponding to a pile temperature range of 10 to 23°C (ΔT of -8°C to 5°C) around a baseline temperature of 18°C. The stable responses of the thermal strains indicate that plastic deformations did not occur in the pile during the daily cyclic temperature changes coupled with the mechanical load in the pile corresponding to 52% of its estimated ultimate capacity. A complex distribution of axial thermal stresses with depth was observed in the pile with higher stress magnitudes near the pile ends particularly at the end of cooling due to larger temperature changes in the cooling cycle. The magnitudes of radial thermal stresses were considerably smaller than the axial thermal stresses along the length of the pile and are not anticipated to play a significant role in the development of thermo-mechanical loads in the pile. The temperatures over the cross-section of the pile were uniformly distributed at the end of cooling and heating at all depths while the axial thermal stresses had a non-uniform distribution but with magnitudes less than the calculated ultimate capacity of the pile.

Keywords: *Energy pile; field tests; thermal responses; building loads; cyclic temperatures.*

Introduction

Energy piles can be subjected to cyclic changes in temperature associated with long-term seasonal ground-source heat pump (GSHP) operation (Brandl, 2006; Murphy and McCartney, 2015; McCartney and Murphy, 2017) and daily intermittent operations of the GSHP (Faizal et al., 2016; 2018). The ground temperatures during daily intermittent operations of the GSHP may recover naturally during non-operating times or could be recharged forcefully using optimized hybrid systems that utilize cooling towers or solar collectors for maintaining a balance of ground temperatures and improving geothermal energy utilization (Yi et al., 2008; Wood et al., 2010). In such hybrid systems, energy piles may encounter frequent cyclic temperature changes that could intensify thermally induced deformations at the pile-soil interface compared to application of monotonic seasonal changes in pile temperature, depending on the magnitude of the axial mechanical load applied at the pile head

(Suryatriyastuti et al., 2013; Olgun et al., 2014; Pasten and Santamarina, 2014). Effects of this cyclic mechanism on the responses of energy piles under building loads are still to be evaluated.

Most of the investigations conducted on field energy piles have focussed on their axial thermal responses when subjected to monotonic heating or cooling (Laloui et al., 2006; Bourne-Webb et al., 2009; Akrouch et al., 2014; Mimouni, 2014; Mimouni and Laloui, 2015; Wang et al., 2015; Murphy et al., 2015; You et al., 2016; Sutman et al., 2017) or under actual heat pump operation (Brandl, 1998, 2006; McCartney and Murphy, 2012; Murphy and McCartney, 2015; McCartney and Murphy, 2017). Of these studies, only a few were conducted on energy piles installed under building loads (Brandl, 2006; Laloui et al., 2006; McCartney and Murphy, 2012; Mimouni and Laloui, 2015; Murphy et al., 2015; Murphy and McCartney 2015; McCartney and Murphy, 2017). Also, the evaluation of the long-term impacts of daily cyclic temperature changes on the thermal response of energy piles in hybrid systems are minimal (Faizal et al., 2016; 2018). The frequent reversals in pile temperatures in hybrid systems compared to normal systems would maintain the pile and ground temperatures closer to undisturbed initial temperatures since the pile and ground temperature changes will always be recovered when the heating and cooling cycles are switched (Yi et al., 2008; Wood et al., 2010). However, it is likely that frequent daily cyclic temperature changes in hybrid systems may lead to much higher cyclic changes in temperature of the pile compared to the surrounding soil due to the relatively low thermal conductivity of most soils. The higher cyclic temperature changes of the pile could lead to a higher expansion and contraction of the pile compared to the surrounding soil, resulting in greater mobilization of side shear stresses due to the possible differential movement of the pile and the soil. Slower changes in temperatures during seasonal operation may, however, lead to volume changes of both the pile and the soil.

Evaluation of radial thermal reactions of energy piles at field scale is scarce (Laloui et al., 2006; Amis et al., 2008; Mimouni, 2014; Mimouni and Laloui, 2015; Wang et al., 2015; Wang, 2017; Faizal et al., 2018), often with conflicting conclusions. For example, the field studies reported by Wang et al. (2015) and Faizal et al. (2018) indicated that radial thermal responses were not significant in comparison to axial thermal responses of the pile, while Mimouni and Laloui (2015) studies suggested that radial thermal responses might be significant. The differences in conclusions from these studies might be due to differences in soil properties encountered on site, and variations in pile construction techniques and pile geometries. Numerical analyses have generally reported that the radial thermal stresses of energy piles are insignificant compared to axial thermal stresses along the length of the pile (Knellwolf et al., 2011; Ozudogru et al., 2015; Gawecka et al., 2017; Chen and McCartney, 2016). Additional investigation is essential to evaluate the impact of daily cyclic temperature changes on the axial and radial thermal responses of energy piles under building loads.

Small-scale physical model studies with thermal cycles on energy piles (Kalantidou et al., 2012; Stewart and McCartney, 2014; Yavari et al., 2014, 2016a; Wang et al., 2017; Nguyen et al., 2017) have indicated that the thermally induced axial settlement of the pile is reversible for pile head loads corresponding to as low as 20% of the ultimate pile capacity, but becomes irreversible for higher pile head loads closer to the ultimate pile capacity. The field tests conducted by Faizal et al. (2018) indicated that the axial and radial thermal responses of an unrestrained energy pile embedded in dense sand followed linear reversible paths for heating and cooling cycles, suggesting that both the pile and the soil did not undergo significant thermally induced deformations. As highlighted in the small-scale physical model studies reported by several investigators (Kalantidou et al., 2012; Stewart and McCartney, 2014; Yavari et al., 2014, 2016a; Wang et al., 2017; Nguyen et al., 2017), it is conceivable that building loads could lead to irreversible axial and radial thermal responses along with associated deformations of the pile and the surrounding soil during cyclic temperature changes. Therefore, further investigations are deemed necessary to evaluate the reversibility of the axial and radial thermal responses of energy piles under building loads when subjected to daily cyclic temperature changes.

Numerical studies reported by Abdelaziz and Ozodugru (2016a, 2016b) and Caulk et al., (2016) have indicated that the presence of non-uniform temperature and axial thermal stress distributions tend to develop over the cross-sectional area of the pile. There are no studies yet on the characterization of the complex distribution of temperatures and axial thermal stresses across the cross-section of energy piles under building loads when subjected to daily cyclic temperature changes.

Based on the gaps in the knowledge noted above, the main aim of this paper is to assess the effects of daily cyclic temperature changes on the axial and radial thermal responses of an energy pile installed under a building. Specifically, the temperature in the energy pile is controlled in a way to simulate the expected changes in temperature that may occur in a hybrid system with forced thermal recharging of the ground temperature. The specific aims of this paper are to assess the reversibility of the axial and radial thermal strains versus the variations in pile temperatures and to evaluate the temperature and axial thermal stress distributions over the cross-section of the energy pile at different depths. For these purposes, an energy pile installed under a 6-story student residential building was subjected to 16 hours of cooling followed by 8 hours of heating, daily, simulating a daily cooling intermittent operation of the pile (i.e. building heating) with scheduled forced ground thermal recovery for a solar-hybrid system. The 8 hours of heating simulates forced thermal recharging of the ground temperature (which would be from a renewable source in an actual hybrid system), which in turn improves the geothermal energy utilization in the following cooling cycle by increasing the temperature gradient between the working fluid and the ground.

Ground Conditions

The soil formation at the site consists of shallow surface sands and silt underlain by very stiff clays, and medium dense to dense clayey and silty sands with increasing depth. The lithology is documented in Table 1, further description of the site is also provided in Barry-Macaulay et al. (2013, 2014). No groundwater was encountered within the depth of the pile during drilling, and the soil was unsaturated.

Energy pile details and experimental procedure

Two cast-in-place bored foundation piles with a diameter of 0.6 m and length of 10 m, from a set of 114 foundation piles for a residential building located at Monash University (Melbourne, Australia), were constructed as energy piles below a ground beam of 800 mm depth and 1200 mm width. One of the two energy piles was instrumented with vibrating wire strain gauges (VWSGs) and thermocouples as shown in the schematic in Figure 1 and was subjected to thermal cycles in this study. Faizal et al (2018b) described in details the instrumentation and installation of these energy piles. In summary, the instrumented energy pile contained 30 VWSGs (model Geokon 4200) installed at five depths of the pile to monitor both axial and radial strains. All the VWSGs were mounted on 30 mm high Styrofoam blocks using cable ties fastened away from the end blocks of the gauges (Figure 2b). The outer axial VWSGs were attached to the reinforcement bars, the central axial VWSGs were attached to the outer side of the tremie guides that housed removable tremies used to pour concrete, and the radial VWSGs were attached to steel bars welded across the diameter of the pile. Further details about the sensors, instrumentation and installation process are documented elsewhere (Faizal 2018; Faizal et al. 2018b). The concrete temperatures were recorded from day two of casting and were observed to reduce with curing time to the magnitudes of the surrounding undisturbed soil temperatures (Bouazza et al. 2015; Singh et al., 2015, Faizal 2018) and were evenly distributed with depth, indicating that the shaft geometry remained uniform with depth without any defects in the concrete.

Faizal et al (2018b) indicated that the four high-density polyethylene U-loops pipes were attached to the inside of the reinforcing cage of the pile, as illustrated in Figure 2a. The nominal concrete cover to the edge of the pipes is 95 mm. The horizontal spacing between the pipes in a given U-loop is about 200 mm. The concrete mix consisted of 7 mm aggregated cement, slag, and fly ash with water to cement ratio of 0.42. The compressive strengths of unreinforced concrete samples were 40 MPa and 62 MPa at 7 and 33 days of installation, respectively, with a modulus of elasticity of 34 GPa at 133 days of installation (Faizal et al., 2018b).

A commercial 2-5 kW Envision geothermal/water source heat pump was used for the experiment. The inlet and outlet of all the U-loops were connected to the inlet and outlet of the heat pump through a plumbing manifold. Type T thermocouples, supplied by ECEFast (Melbourne, Australia), recorded the fluid temperatures at the inlet and outlet of each

U-loop. The fluid flow rates were recorded using TM series digital water flowmeters installed at the inlet and outlet of the plumbing manifold. Data from the thermocouples and the VWSGs were logged using Pico Technology’s USB-TC08 data loggers and Campbell Scientific CR1000 data loggers, respectively (Faizal et al., 2018b).

The cyclic cooling and heating experiment was conducted for 17 days at a fluid flow rate of approximately 16 litres per minute. The fluid returning from the piles exited into a buffer tank installed at the inlet of the heat pump. A Fernox Alphi-11 antifreeze protector was added to the water (at approximately 25% of the total volume of water in the system) to ensure that water did not freeze and block the pipelines during the cooling cycles. All the four U-loops in the pile were thermally active giving an even heat exchanger layout in the pile. The four U-loops in the pile were connected in series where the fluid flowed successively in each loop from the inlet of the first loop to the outlet of the fourth loop. The pile was cooled for 16 hours followed by heating for 8 hours, daily. There were some performance issues of the heat pump in the first cooling cycle which disrupted cooling temperatures for up to 10 hours. Once this was resolved, the cooling cycle was restarted for 16 hours. Hence, the total time for the first cooling cycle is 26 hours, while the other cooling cycles were 16 hours followed by 8 hours heating. No other issues were encountered for the duration of the experiment. The fluid inlet and outlet temperatures recorded at the pile head consistently cycled between approximately 8 to 30°C, as shown in Figure 3a. The range of temperatures for energy piles during operation has been reported to be approximately between 10 to 35°C depending on the usage requirement (Brandl, 2006; McCartney and Murphy, 2012; Murphy and McCartney, 2015; McCartney and Murphy, 2017). The change in fluid temperatures were approximately -2.5°C at the end of cooling and 3°C at the end of heating, as shown in Figure 3b.

Results and discussions

Time series of temperatures and thermal strains

The thermal strains, ε_T, were calculated using the calibration factors of the VWSGs and by correcting for temperature changes, as follows (Faizal et al., 2018b):

$$\varepsilon_T = (\varepsilon_i - \varepsilon_o) B + (T_i - T_o) \alpha_s \quad (1)$$

where ε_i is strain at time *i*, ε_o is the reference strain and is selected at the beginning of the thermal cycles, and hence the calculated thermal strains neglects the effects of building loads, *B* is the batch calibration factor of the strain gauges with a magnitude of 0.975, T_i is the temperature of the strain gauges at time *i*, T_o is the reference temperature of the strain gauges, α_s is the coefficient of linear thermal expansion of steel wire in the strain gauges (12.2 με/°C). The strains ε_i and ε_o were calculated as follows:

$$\varepsilon = G\left(f^2 \times 10^{-3}\right) \quad (2)$$

where f is the resonant frequency of the strain gauges at the reference or at time i, and G is the gauge factor with a magnitude of 3.304.

The time series of the pile temperatures and change in pile temperatures recorded from the axial and radial VWSGs are presented in Figure 4. Average magnitudes of pile temperatures and thermal strains from the axial VWSGs are considered for ease of comparison with pile temperatures and thermal strains from radial VWSGs. The temperatures plotted in Figure 4 are for depths below 3 m to compare between the axial and radial thermal responses, as the radial VWSG at a depth of 1.36 m was damaged and did not provide any data on the radial thermal strains. One of the axial VWSGs at 1 m depth was also damaged and did not provide any data on the variation of axial thermal strains. The axial thermal responses against depth are presented later in the paper. The pile temperatures (including change in pile temperatures) recorded from the axial and radial VWSGs (Figure 4) showed similar magnitudes with slight differences at the end of heating/cooling cycles between consecutive days. The pile temperatures at the end of heating and cooling are above and below the initial undisturbed pile temperatures of approximately 18°C recorded prior to the experiments, respectively; hence the ΔT magnitudes cycled between positive and negative magnitudes. The pile temperatures cycled approximately between 10°C and 23°C and the change in pile temperatures, ΔT, cycled approximately between -8°C and 5°C.

The time series of axial and radial thermal strains below a depth of 3 m is shown in Figure 5. Similar to the ΔT magnitudes, the thermal strains also cycled between positive and negative magnitudes. The ranges of magnitudes of radial thermal strains are generally larger than the range of magnitudes of axial thermal strains at all depths, indicating an overall higher restriction to thermal expansion/contraction of the pile in the axial direction.

The largest difference in the magnitudes between the axial and radial thermal strains at the end of heating and cooling is at an approximate depth of 3 m (axial and radial strains at depths of 3.05 m and 3.3 m, respectively) (Figure 5a), which is possibly the location of the null point as the range of magnitudes of the axial thermal strains are also the lowest at this depth. The axial thermal strains are lower than the radial thermal strains at the end of cooling and heating at this depth, indicating that the energy pile is more restrained to axial thermal expansion and contraction. The null point or the neutral plane is the location in the pile where ideally the thermally induced axial displacemnt is zero and the axial thermal stress is the maximum. The thermally induced axial displacements and moblised side shear stresses act in opposite vertical directions from this point to ensure vertical equilibrium (Bourne-Webb et al. 2009; Amatya et al. 2012; Bourne-Webb et al. 2013). The axial and radial thermal strains at depths of 5 m and 5.3 m, respectively, show similar magnitudes (hence, same restriction) at the end of cooling, while the axial thermal strains are more restrained at the end of heating (Figure 5b). The axial thermal strains at a depth of 7.28 m (Figure 5c) is more restricted than radial thermal strains at a depth of 7.46 m at the end of heating, while the radial thermal strains are more restricted than axial thermal strains at the end of cooling. The axial thermal strains at a depth of 9.5 m are more restricted than the radial thermal strains at a depth of 9.25 m at the end of cooling but show similar magnitudes at the end of heating.

The results of the daily cyclic pile temperature changes presented by Faizal et al. (2018) at a single depth for an unrestrained field-scale energy pile installed in dense sand and subjected to a temperature change of -10°C to 22.5°C indicated that the axial thermal strains were more restricted to thermal expansion/contraction than the radial thermal strains. The results of Figure 5, however, indicate that depending on the location in the energy pile under building loads, the radial thermal strains may not always show lower restrictions to thermal expansion or contraction at the end of heating or cooling when the pile is subjected to daily cyclic temperature changes. The range of temperature changes of the energy pile in the present study compared to the study of Faizal et al. (2018a, b) is, however, relatively low (i.e. approximately - 8°C to 5°C in the present study). This could have prevented the radial thermal strains from fully developing in the pile.

Thermal responses to change in pile temperatures

The variations of the axial and radial thermal strains versus the change in pile temperatures, ΔT, at four-day intervals are shown in Figure 6. The observed linear trends confirm that the range of magnitudes of the axial thermal strains is lower than the range of magnitudes of the radial thermal strains for a similar range of pile temperature changes (i.e. approximately -8°C to 5°C). The axial thermal strains follow almost linear reversible paths against the variation in cyclic pile temperatures for daily heating and cooling cycles, at all depths. There is, however, an initial ratcheting behaviour observed mostly in the radial thermal strains between 3.3 m to 7.46 m, the highest being at 7.46 m (Figure 6b, 6d, and 6f). This initial ratcheting behavior, which reduced with operating time as thermal strains stabilized towards the end of the experiment, possibly occurred due to high initial heat dissipation into the surrounding sand resulting from high initial thermal gradient between the inlet fluid and the ground. Although plastic deformations is unlikely to have occurred, the behavior of radial thermal responses at a depth of 7.46 m shown in Figure 6f would require further long-term simulations to fully evaluate if any plastic deformations occurred at the pile-soil interface at that location. However, as discussed later in the paper, the magnitudes of radial thermal stresses developed in the energy pile are negligible compared to axial thermal stresses, hence radial thermal effects on the pile-soil interface would also be very low compared to axial thermal effects.

The results shown in Figure 6 indicate that the load of the building does not have any significant impact on the reversibility of the axial thermal strains for frequent cyclic temperature changes of the pile. The calculated ultimate capacities of compressive and tension mechanical loads are 2701 kN (9.6 MPa) and 2157 kN (7.6 MPa), respectively (Faizal et al., 2018b). The design compressive and tension axial working mechanical loads of the 10 m long, 0.6 m diameter energy pile with a factor of safety of 1.9 are 1404 kN (4.96 MPa) and 1122 kN (3.97 MPa), respectively (Faizal et al., 2018b). The design pile head load is thus approximately 52% of the calculated ultimate pile head load and the results shown in Figure 6 indicate that the thermal strains are reversible for frequent cyclic temperature changes at this working load ratio of the energy pile for the duration of the experiment. The current results are different from the findings reported for small-scale model studies due to differences in soil types and preparation techniques and differences in boundary conditions since field installations represent actual effects of the surrounding soil and pile installation effects compared to idealized installations in small-scale studies.

The thermal strains are reversible for daily cyclic temperature changes of the pile likely due to its adequate design factor of safety which considers the mechanical loads imposed by the building as well as the thermal loads induced in the pile for the range of temperatures studied. The type of soil also plays an essential role in the thermal response of the energy pile. It is likely that the dense sand at this site has also contributed to the reversible axial and radial thermal responses of the energy pile by providing a higher resistance to thermal expansion and contraction. As has also been shown in numerical studies, the settlement of energy piles is much lower in dense sand than in loose sand due to differences in the shaft friction (Saggu and Chakraborty, 2015). The linear reversible paths of the thermal strains at all depths indicate that any temperature induced relative settlements between the pile and the soil was reversible.

Evaluation of thermal responses against depth

The profiles of temperatures, variation in temperatures, and axial and radial thermal strains plotted against depth at four-day intervals are shown in Figure 7. The pile temperatures and variation in pile temperatures shown in Figure 7a to Figure 7d indicate that the sixteen-hour cooling cycle imposed larger pile temperature variations (ΔT up to -9°C) than the eight-hour heating cycle (ΔT up to 5°C). The temperatures return to similar magnitudes at the end of heating and cooling (apart for Day 4 where the heat pump imposed higher temperatures during heating).

The axial thermal strains at the end of cooling in Figure 7e show larger variations with depth compared to the end of heating, likely due to larger changes in pile temperatures during the cooling cycle. The most significant restriction to axial thermal strains at the end of cooling is at a depth of 3.05 m, possibly the location of the null point where ideally the axial thermal stresses are the maximum. The pile toe also appears to provide resistance to axial thermal strains at the end of cooling, leading to a complex distribution of axial thermal strains with depth. The restraints provided by the building on the pile head and by the dense sand on the toe could have provided differing stiffness at each end of the pile which could have affected the axial thermal load distribution in the pile during temperature cycles (Bourne-Webb et al., 2013). Locations of high restrictions in axial thermal strains are not evident with depth at the end of heating likely due to the lower pile temperature changes imposed in the heating cycle.

The cyclic pile temperature changes also affected the distribution of the radial thermal strains with depth, particularly at a depth of 7.46 m. The radial thermal strains at 7.46 m are unexpectedly lower than the axial thermal strains at a depth of 7.28 m at the end of cooling. This was, however, not observed at the end of heating. The magnitudes of radial thermal strains at other depths shown in Figure 7f are either similar or larger than the magnitudes of axial thermal strains at the end of cooling or heating, confirming that radial thermal strains may not always show lower restrictions than axial thermal strains for an energy pile under building loads subjected to the range of daily cyclic temperatures reported in this paper.

The thermal and thermo-mechanical stresses developed in the pile are shown in Figure 8. The tensile stresses developed during cooling and compressive stresses developed during heating are deemed to be positive and negative, respectively. The thermal stresses, which develop when the free thermal expansion/contraction of the energy pile is restricted by the soil-structure interaction, are a function of the modulus of the pile and can be estimated as follows (Amatya et al., 2012; Murphy et al., 2015; Caulk et al., 2016):

$$\sigma_T = E_p \left(\varepsilon_T - \varepsilon_{free} \right) \tag{3}$$

where E_p is the Young's modulus of the concrete, ε_T is the actual thermal strains measured in the pile calculated using equation 1, and $\varepsilon_{free}$is the free thermal expansion of the pile estimated by multiplying the change in pile temperature , ΔT, and the coefficient of thermal expansion of the concrete, α_c.

Upon calculation of the free thermal strains using an average value of α_c = 13 με /°C and the ΔT magnitudes shown in Figure 7c and Figure 7d, it was found that the actual radial thermal strains measured in the pile exceeded the free radial thermal strains, particularly at the end of heating. This could be credited to the transient effects of temperature reversals between positive and negative magnitudes which has been previously identified to cause issues in estimating thermal stresses

(Murphy and McCartney, 2015; Faizal et al., 2018). Another reason could be the temperature recorded by the gauge that is used to estimate the thermal stresses is different from the average temperature of the pile (Murphy and McCartney, 2015). For the sake of simplicity in the analysis, the axial thermal stresses were estimated using Equation 3 whereas a cavity expansion analysis (Equation 4) was used to estimate the radial thermal stresses in the pile since the mobilized radial pile-soil contact stresses, σ_n, are equal to the radial thermal stresses developed in the pile for radial stress equilibrium (Faizal et al., 2018):

$$\sigma_n = \frac{E_s}{1+v_s}\frac{\Delta r}{r} \quad (4)$$

Where r is the radius of the pile, Δr is the thermally induced radial displacement of the pile, Δr/r is assumed to be equal to the radial thermal strain for a given change in temperature, and E_s and v_s are the Young's modulus and Poisson's ratio of the surrounding dense sand, respectively (assumed to be 60 MPa and 0.3, respectively, based on typical values for dense sand, Faizal et al , 2018b). This simple model with a constant stiffness is used to estimate the moblized radial pile-soil contact stresses (and hence the radial thermal stresses developed in the pile) since the thermally induced radial pile displacement, Δr, is relatively small compared to the initial pile radius and the shear strength of sand is not expected to be affected by temperature variations (Barry-Macaulay, 2013; Donna et al., 2015; Yavari et al., 2016b).

The axial thermal stresses developed in the pile at the end of cooling and heating are plotted together with the mechanical stresses imposed by the load of the building in Figure 8a. The mechanical stresses are the vertical stress distribution of the building load along the length of the pile, and are estimated from the variations in strains during building construction times the modulus of elasticity of the pile. The magnitudes reduce with depth as the building load is taken up by the shaft friction, with minimal effects at the pile toe. There is a change in soil profile at a depth of 3.5 m which could have affected the mechanical stress distribution at that location. The sign convention in the present paper is that compressive and tensile stresses are considered as negative and positive, respectively. The magnitudes of tensile axial thermal stresses at the end of cooling are larger than the compressive axial thermal stresses at the end of heating, due to differences in ΔT magnitudes shown in Figure 7c. Also, the axial thermal stresses at the end of cooling show larger variations with depth due to larger changes in the axial thermal strains with depth at the end of cooling, shown in Figure 7e. The radial thermal stresses presented in Figure 8b are significantly lower (up to 0.004 MPa) than the axial thermal stresses (up to 2.5 MPa) developed in the pile and are not expected to modify the radial mechanical loads imposed by the building. This low magnitude of radial thermal stresses indicates that the radial thermal effects do not contribute significantly to the development of axial thermal strains and stresses in the pile. Radial thermal stresses in energy piles have also been reported to have significantly low magnitudes in numerical studies (Olgun et al., 2014; Ozudogru et al., 2015; Gawecka et al., 2017) and field studies (Faizal et al., 2018). The study on an unrestrained energy pile installed in dense sand conducted by Faizal et al. (2018) reported axial and radial thermal stresses up to 3 MPa and 0.012 MPa, respectively. Gawecka et al. (2017) numerically back analyzed the Lambeth College field energy pile installed in London clay with a 1200 kN head load (studied by Bourne-Webb et al., 2009) and reported axial and radial thermal stresses ranging from approximately 5 – 0.5 MPa and 0.01 – 0.03 MPa from the head to the toe of the pile, respectively. Ozudogru et al. (2015) conducted a numerical study on an energy pile embedded in cohesive soil and without head loads and also reported that the radial stresses were small in magnitude (≈ 0.005 MPa) compared to the axial thermal stresses (≈ 0.55 MPa). The radial thermal stresses for a plane-stress (floating) and plane-strain (fixed at the top and bottom) energy pile in a numerical analysis performed by Olgun et al. (2014) was reported to be lower than 15 kPa and was concluded to be insignificant in causing thermally induced changes at the pile-soil interface.

The axial thermo-mechanical stresses, which are the total of the axial mechanical stresses imposed by the load of the building and the axial thermal stresses developed in the pile, are shown in Figure 8c. The largest axial thermo-mechanical stresses at the end of heating are -4.3 MPa at the pile head and -0.3 MPa near the toe. The largest thermo-mechanical stresses at the end of cooling are - 3.2 MPa at the pile head and 1.2 MPa near the toe. The magnitudes of these stresses are lower than the ultimate compressive, and tensile capacities of the pile, hence the range of frequent cyclic pile temperature changes reported in this paper are not expected to lead to any temperature-induced change in the capacity of the pile.

Cross-sectional distribution of temperatures and axial thermal stresses

The variation of pile temperatures and axial thermal stresses over the cross-sectional area of the pile at all depths, obtained from the individual axial VWSGs, are presented in Figure 9 and Figure 10, respectively. The locations of the axial VWSGs are non-dimensionalized with respect to the radius of the pile. The axial VWSGs at locations V1 and V2, displayed in Figure 1, correspond to the non-dimensionalized radius of -0.47, V5 corresponds to the centre of the pile, and V3 and V4 correspond to the non-dimensionalized radius of 0.47. The results are presented at end of heating and cooling for Day 4 and Day 8. Similar trends were observed for other days.

The pile temperature variations shown in Figure 9 are highest near the pile toe at a depth of 9.5 m (Figure 9e) with a variation of up to 3.3°C at the end of heating, probably due to the cluster of U-bends causing turbulence in the pipes. The pile temperatures at other depths shown in

Figure 9a to Figure 9d are within a low range of magnitudes of 0.2°C to 1.1°C, indicating that uniform temperature distributions across the cross-section of the energy pile with even heat exchanger layout could be considered for design purposes for the range of cyclic temperatures studied in this paper.

The frequent temperature reversals develop non-uniform axial thermal stress distributions over the planar cross-section of the energy pile at all depths, as indicated in Figure 10. The axial thermal stresses at one of the locations at a depth of 1 m is not calculated as the VWSG (EV3) at this location was damaged and did not provide any data on the axial thermal strains (Figure 10a). The largest variations in axial thermal stresses over the cross-section of the pile are observed near the pile ends, particularly near the pile toe at a depth of 9.5 m (Figure 10e) where the range of magnitudes of axial thermal stresses is approximately 2.5 MPa at the end of cooling. The results indicate that pile end restraint leads to higher non-uniformities in axial thermal stress distributions for cyclic temperature changes. The range of magnitudes of axial thermal stresses at other depths shown in Figure 10a to Figure 10d are within a low range of ± 1.7 MPa. The magnitudes of the axial thermal stresses at any location of the cross-section at the end of cooling or heating are however within the ultimate capacities of the pile, and thus the non-uniform stress distribution is not expected to cause any temperature-induced changes in the capacity of the pile. Further simulation studies are warranted to verify and extrapolate thermal stress contours over the cross-section of the energy pile and better identify regions of high-stress concentration, especially near the HDPE pipes where the concrete temperatures will be highest or lowest. Further investigations are also required to gauge the likelihood of concrete micro-cracking from frequent temperature reversals of the energy pile, even though it is not expected to occur in reinforced concrete.

Conclusions

This paper assessed the impact of daily cyclic temperature variations on the axial and radial thermal responses of an energy pile installed under a six-story building. For a pile design to ultimate head load ratio of 52% and for pile temperature changes of -8°C to 5°C, the axial thermal strains followed linear reversible paths along the length of the pile for daily thermal cycles, indicating that frequent cyclic temperature variations coupled with the load of the built structure did not result into thermally induced plastic deformations for the cast-in-place energy pile installed in dense sand studied in this paper. Some initial ratechting behaviour was observed in the radial thermal strains which stablized towards the end of the experiment. The magnitudes of radial thermal stresses were found to be insignificant in comparison to axial thermal stresses developed in the pile at all depths indicating that radial thermal expansion/contraction of the pile does not have major impact on the skin friction of the pile. The temperature distribution over the cross-section of the pile at the end of cooling and heating indicated that a low range of variations was achieved at all depths and can be considered to be uniformly distributed for design purposes for energy piles with even heat exchanger layouts installed in dense sand. The axial thermal stresses were non-uniformly distributed across the cross-section of the pile at the end of cooling and heating for all depths, but the magnitudes were within the ultimate capacities of the pile. The results presented in this paper are for a single energy pile. Further studies are required to evalaute the effects of cyclic temperature changes on multiple energy piles installed under built structures that better represent real operating conditions.

Acknowledgements

This research project is supported under the Australian Research Council's Linkage Projects funding scheme (project number LP120200613). The authors also acknowledge the Australian Government Research Training Program Scholarship provided to the first author. The US National Science Foundation grant CMMI-0928159 supported the third author. The support of all the sponsors is gratefully acknowledged.

References

Abdelaziz, S. L. and Ozudogru, T. Y. (2016a). "Selection of the design temperature change for energy piles." *Applied Thermal Engineering*, 107, 1036-1045.

Abdelaziz, S. and Ozudogru, T.Y. (2016b). “Non-uniform thermal strains and stresses in energy piles.” *Environmental Geotechnics*, 3(4), 237-252.

Akrouch, G., Sánchez, M. and Briaud, J-L. (2014). “Thermo-mechanical behavior of energy piles in high plasticity clays.” *Acta Geotechnica*, 9(3), 399-412.

Amatya, B. L., Soga, K., Bourne-Webb, P. J., Amis, T. and Laloui, L. (2012). “Thermo-mechanical behaviour of energy piles.” *Géotechnique*, 62(6), 503-519.

Amis, T., Bourne-Webb, P.J., Davidson, C., Amatya, B., and Soga, K. (2008). "The effects of heating and cooling energy piles under working load at Lambeth College, UK." *33rd Annual and 11th Intl. Conf. of the Deep Foundations* Institute, New York, USA.

Barry-Macaulay, D. (2013). “An investigation on the thermal and thermo-mechanical behaviour of soils.” Master of Engineering Thesis, Department of Civil Engineering, Monash University, Melbourne, Australia.

Barry-Macaulay, D., Bouazza, A., Singh, R. M., Wang, B., and Ranjith, P. G. (2013). Thermal conductivity of soils and rocks from the Melbourne (Australia) region. *Engineering Geology*, 164, 131-138.

Barry-Macaulay, D., Bouazza, A., Singh, R. M., and Wang, B. (2014). Thermal properties of Victorian soil and rock. *Australian Geomechanics Journal*, 49(2), 31-44.

Bouazza A., Singh R.M. and Faizal M. (2015). “Full scale geothermal energy pile studies at Monash University, Melbourne, Australia". *Thermoactive foundations for sustainable buildings*, McCartney, J.S., Krarti, M., Kwag, B.C., Bouazza, A., Singh, R.M. and Faizal, M. American Society of Mechanical Engineers (ASME), New York. pp 95-117.

Bourne-Webb, P. J., Amatya, B., Soga, K., Amis, T., Davidson, C. and Payne, P. (2009). "Energy pile test at Lambeth College, London: geotechnical and thermodynamic aspects of pile response to heat cycles." *Géotechnique*, 59(3), 237-248.

Bourne-Webb, P. J., Amatya, B., and Soga, K. (2013). "A framework for understanding energy pile behaviour." *Proceedings of the Institution of Civil Engineers - Geotechnical Engineering*, 166(2), 170-177.

Brandl, H. (1998). "Energy piles and diaphragm walls for heat transfer from and into the ground." In *Proceedings of the 3rd International Geotechcnial Seminar on Deep Foundations on Bored and Auger Piles, Ghent, Belgium*, edited by W.F. Van Impe and W. Haegeman, 37 -60. Rotterdam/Brookfield: A.A. Balkema.

Brandl, H. (2006). "Energy foundations and other thermo-active ground structures." *Géotechnique*, 56(2), 81-122.

Caulk, R., Ghazanfari, E., and McCartney, J.S. (2016). "Parameterization of a calibrated geothermal energy pile model." *Geomechanics for Energy and the Environment*, 5(3), 1-15.

Chen, D. and McCartney, J.S. (2016). "Parameters for load transfer analysis of energy piles in uniform nonplastic soils." *International Journal of Geomechanics*, 17 (7), 10.1061/(ASCE)GM.1943-5622.0000873, 04016159-1-17.

Donna, A.D., Ferrari, A., and Laloui, L. (2015). “Experimental investigations of the soil–concrete interface: physical mechanisms, cyclic mobilization, and behaviour at different temperatures.” *Canadian Geotechnical Journal*, 53(4), 659-672.

Faizal, M. (2018). “Axial and radial thermal responses of field-scale energy piles”. PhD Thesis, Department of Civil Engineering, Monash University, Melbourne, Australia.

Faizal, M., Bouazza, A. and Singh, R. M. (2016). “An experimental investigation of the influence of intermittent and continuous operating modes on the thermal behaviour of a full scale geothermal energy pile.” *Geomechanics for Energy and the Environment*, 8, 8-29.

Faizal, M., Bouazza, A., Haberfield, C. and McCartney, J.S. (2018a). “Axial and radial thermal responses of a field scale energy pile under monotonic and cyclic temperature changes”. *Journal of Geotechnical and Geoenvironmental Engineering*, 144(10), 04018072. doi: 10.1061/(ASCE)GT.1943-5606.0001952..

Faizal, M., Bouazza, A., McCartney, J.S, and Haberfield, C. (2018b). “Axial and radial thermal responses of an energy pile under a 6-storey residential building”. *Canadian Geotechnical Journal*. doi.org/10.1139/cgj-2018-0246.

Gawecka, K. A., Taborda, D. M. G., Potts, D. M., Cui, W., Zdravković, L., and Kasri, M. S. H. (2017). “Numerical modelling of thermo-active piles in London Clay.” *Proceedings of the Institution of Civil Engineers - Geotechnical Engineering*, 170(3), 201-219.

Kalantidou, A., Tang, A. M., Pereira, J-M. and Hassen, G. (2012). “Preliminary study on the mechanical behaviour of heat exchanger pile in physical model.” *Géotechnique*, 62(11), 1047-1051.

Knellwolf, C., Peron, H., and Laloui, L. (2011). “Geotechnical analysis of heat exchanger piles.” *Journal of Geotechnical and Geoenvironmental Engineering*, 130 (10), 10.1061/(ASCE)GT.1943-5606.0000513, 890–902.

Laloui, L., Nuth, M. and Vulliet, L. (2006). “Experimental and numerical investigations of the behaviour of a heat exchanger pile.” *International Journal for Numerical and Analytical Methods in Geomechanics*, 30(8), 763-781.

McCartney, J. S. and Murphy, K. D. (2012). “Strain distributions in full-scale energy foundations.” *DFI Journal: The Journal of the Deep Foundations Institute*, 6(2), 26-38.

McCartney, J.S. and Murphy, K.D. (2017). “Investigation of potential dragdown/uplift effects on energy piles.” *Geomechanics for Energy and the Environment*, 10, 21-28.

Mimouni, T. (2014). “Thermomechanical characterization of energy geostructures with emphasis on energy piles.” PhD thesis, Laboratory of Soil Mechanics, École Polytechnique Fédérale de Lausanne, Lausanne, Switzerland.

Mimouni, T. and Laloui, L. (2015). “Behaviour of a group of energy piles.” *Canadian Geotechnical Journal*, 52(12), 1913-1929.

Murphy, K. D. and McCartney, J. S. (2015). “Seasonal response of energy foundations during building operation.” *Geotechnical and Geological Engineering*, 33(2), 343-356.

Murphy, K. D., McCartney, J. S., and Henry, K. S. (2015). “Evaluation of thermo-mechanical and thermal behavior of full-scale energy foundations.” *Acta Geotechnica,* 10(2), 179-195.

Nguyen, V. T., Tang, A. M., and Pereira, J.-M. (2017). “Long-term thermo-mechanical behavior of energy pile in dry sand.” *Acta Geotechnica*, 12(4), 729-737.

Olgun, C.G., Ozudogru, T. Y. and Arson, C. F. (2014). “Thermo-mechanical radial expansion of heat exchanger piles and possible effects on contact pressures at pile–soil interface.” *Géotechnique Letters*, 4(3), 170-178.

Ozudogru, T.Y., Olgun, C.G., and Arson, C.F. (2015). “Analysis of friction induced thermo-mechanical stresses on a heat exchanger pile in isothermal soil.” *Geotechnical and Geological Engineering*, 33(2), 357-371.

Pasten, C., and Santamarina, J. (2014). “Thermally induced long-term displacement of thermoactive piles.” *Journal of Geotechnical and Geoenvironmental Engineering,* 10.1061/(ASCE)GT.1943-5606.0001092, 06014003.

Saggu, R. and Chakraborty, T. (2015). “Cyclic thermo-mechanical analysis of energy piles in sand.” *Geotechnical and Geological Engineering*, 33(2), 321-342.

Singh, R. M., Bouazza, A., and Wang, B. (2015). “Near-field ground thermal response to heating of a geothermal energy pile: Observations from a field test.” *Soils and Foundations*, 55(6), 1412-1426

Stewart, M. A. and McCartney, J. S. (2014). “Centrifuge modeling of soil-structure interaction in energy foundations.” *Journal of Geotechnical and Geoenvironmental Engineering*, 10.1061/(ASCE)GT.1943-5606.0001061, 04013044-1-11.

Suryatriyastuti, M. E., Mroueh, H. and Burlon, S. (2013). “Numerical analysis of the bearing capacity in thermo-active piles under cyclic axial loading.” Energy geostructures: Innovation in underground engineering, Laloui, L. and Donna, A.D., eds., John Wiley, Hoboken, NJ, 139–154.

Sutman, M., Olgun, G., Laloui, L., and Brettmann, T. (2017). “Effect of end-restraint conditions on energy pile behavior.” *Geotechnical Frontiers 2017*, Florida, USA, 165-174.

Wang, B. (2017). “Behaviour of pile foundations subjected to thermal loading.” Master of Engineering Thesis, Department of Civil Engineering, Monash University, Melbourne, Australia.

Wang, B., Bouazza, A., Singh, R., Haberfield, C., Barry-Macaulay, D. and Baycan, S. (2015). “Posttemperature effects on shaft capacity of a full-scale geothermal energy pile.” *Journal of Geotechnical and Geoenvironmental Engineering*, 141 (4), 10.1061/(ASCE)GT.1943-5606.0001266, 04014125-1-12.

Wang, C., Liu, H., Kong, G., and Ng, C. W. W. (2017). “Different types of energy piles with heating–cooling cycles.” *Geotechnical Engineering*, 170(3), 220-231.

Wood, C. J., Liu, H. and Riffat, S. B. (2010). “Comparison of a modelled and field tested piled ground heat exchanger system for a residential building and the simulated effect of assisted ground heat recharge.” *International Journal of Low-Carbon Technologies*, 5(3), 137-143.

Yavari, N., Tang, A. M., Pereira, J.M. and Hassen, G. (2014). “Experimental study on the mechanical behaviour of a heat exchanger pile using physical modelling.” *Acta Geotechnica*, 9(3), 385-398.

Yavari, N., Tang, A. M., Pereira, J.M. and Hassen, G. (2016a). “Mechanical behaviour of a small-scale energy pile in saturated clay.” *Géotechnique*, 66(11), 878-887.

Yavari, N., Tang, A. M., Pereira, J.M., and Hassen, G. (2016b). "Effect of temperature on the shear strength of soils and the soil–structure interface." *Canadian Geotechnical Journal*, 53(7), 1186-1194.

Yi, M., Hongxing, Y. and Zhaohong, F. (2008). “Study on hybrid ground-coupled heat pump systems.” *Energy and Buildings*, 40(11), 2028-2036.

You, S., Cheng, X., Guo, H., and Yao, Z. (2016). “Experimental study on structural response of CFG energy piles.” *Applied Thermal Engineering*, 96, 640-651.

Table 1. Summary of ground conditions at the test site.

Depth (m)	Soil type	Soil description	In-situ test values	Gravimetric water content (%)
0 – 0.4	Fill material	Crushed rock silt, sand, moist, medium dense	–	–
0.4 – 3.5	Sandy clay	Silt, sand (sand lenses) moist, stiff - very stiff	S: 90 – 140 kPa SPT N: 12 - 27	13 – 24
3.5 – 12.5	Sand	Sand, clay	SPT N: 25 – 30	5 – 13

	lenses, silt, cemented lenses, moist, dense	

S: Vane shear strength.

SPT N: Standard penetration test blow count.

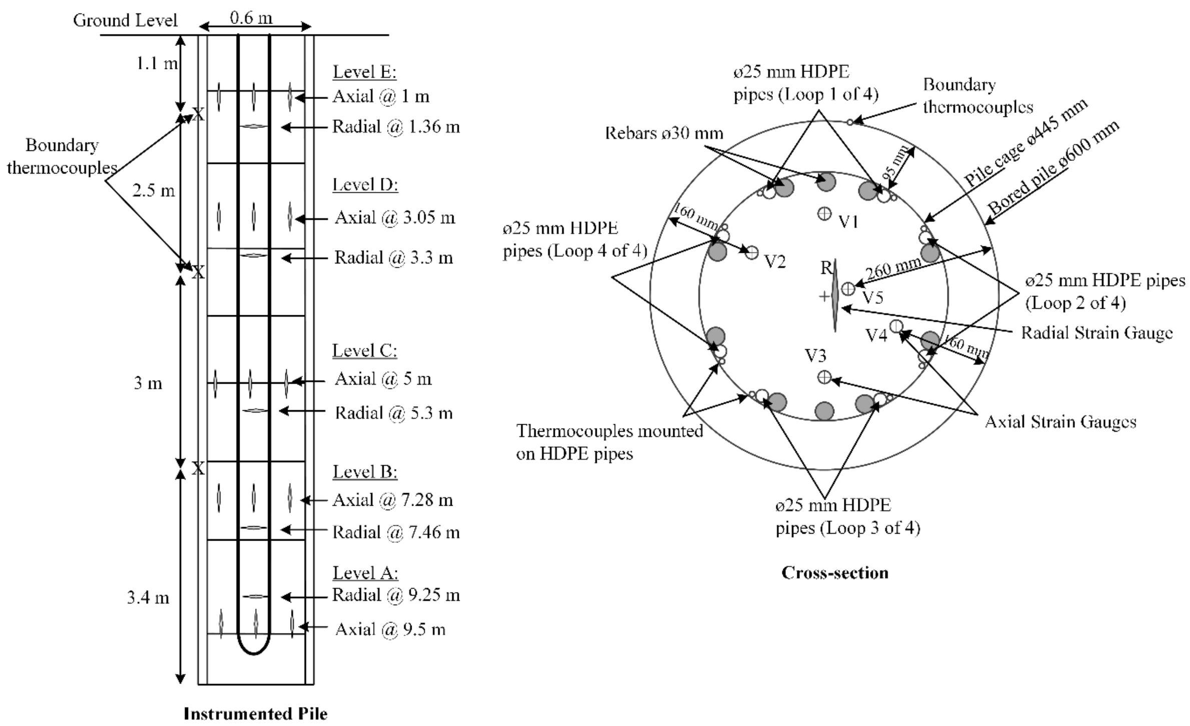

Figure 1. Schematic of the instrumented energy pile and a typical cross section showing the location of sensors at each depth.

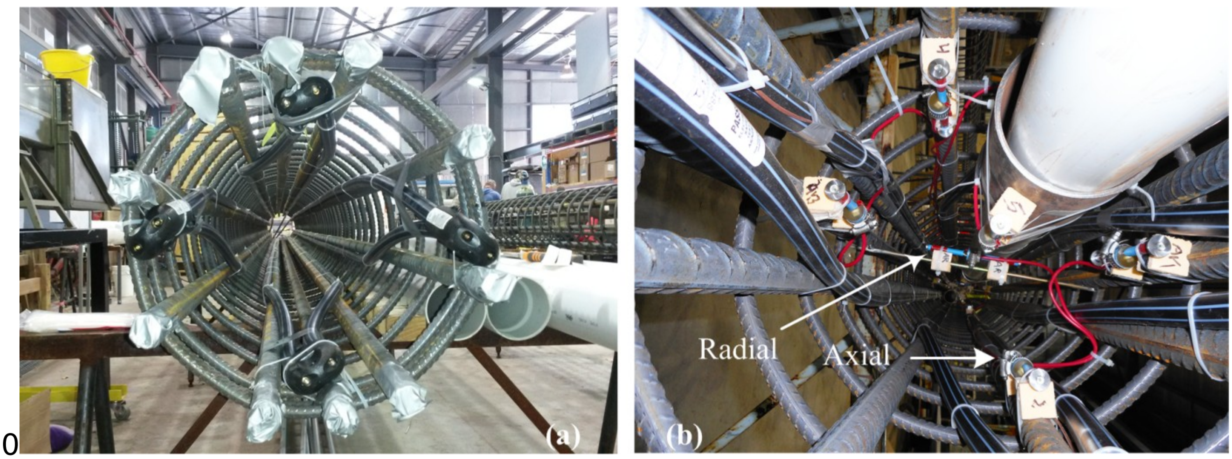

Figure 2. Images of the experimental setup: a) U-loops inside the energy pile cage b) axial and radial VWSGs inside the energy pile cage near the pile toe.

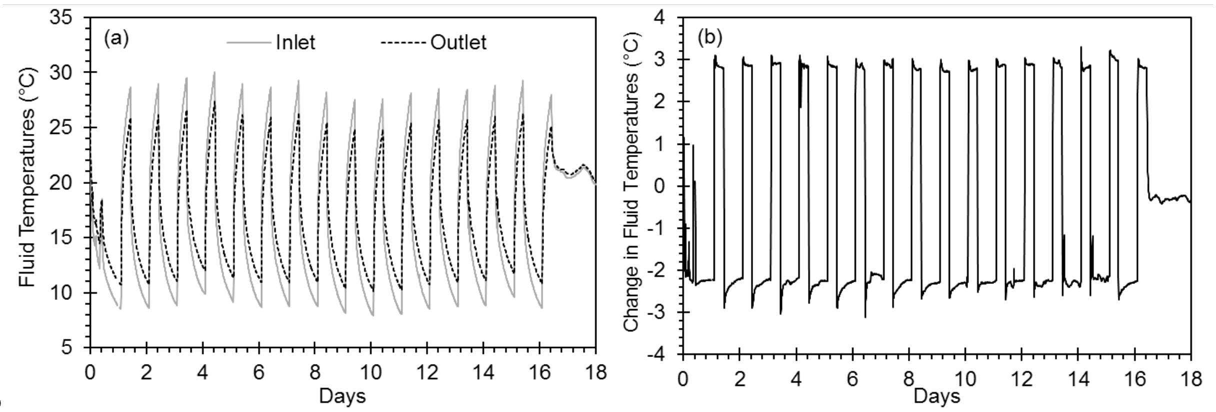

Figure 3. Fluid temperatures: a) at the inlet and outlet b) change in fluid temperatures.

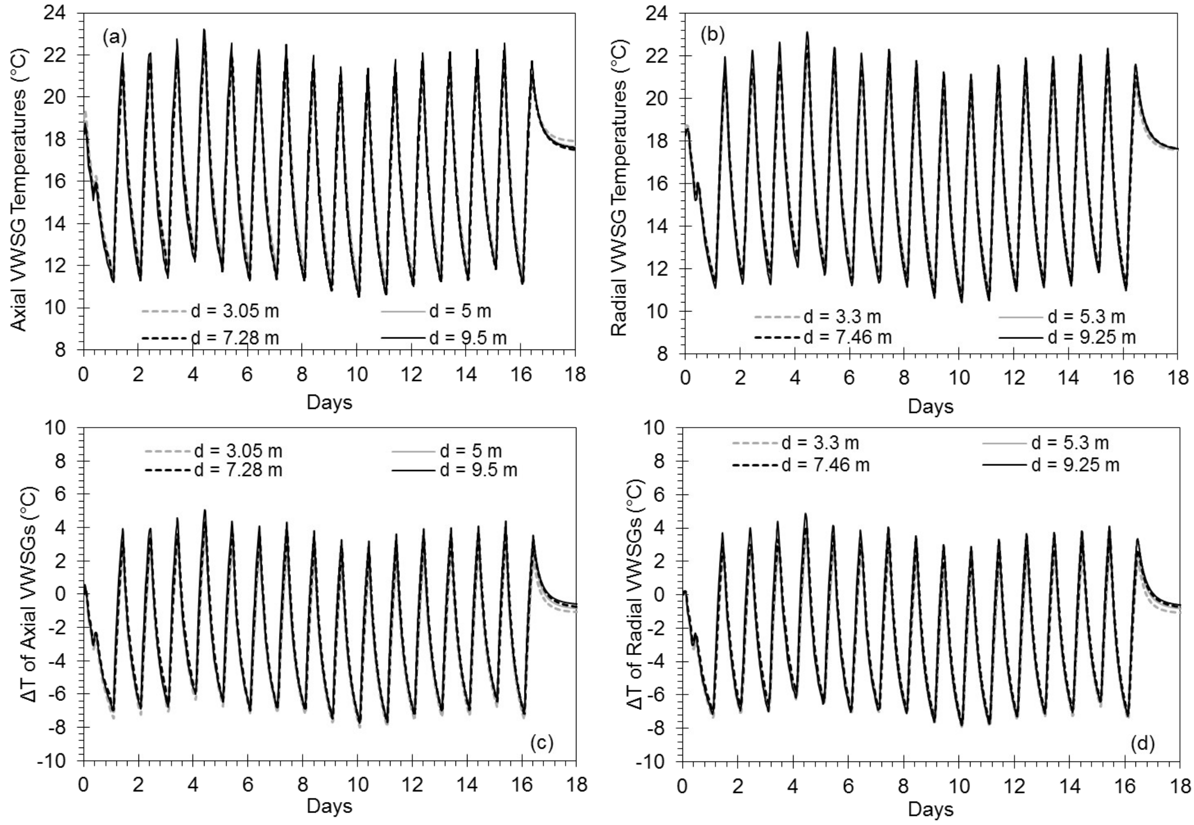

Figure 4. Time series of pile temperatures: a) pile temperatures from axial VWSGs b) pile temperatures from radial VWSGs c) change in pile temperatures, *ΔT*, from axial VWSGs d) change in pile temperatures, *ΔT*, from radial VWSGs.

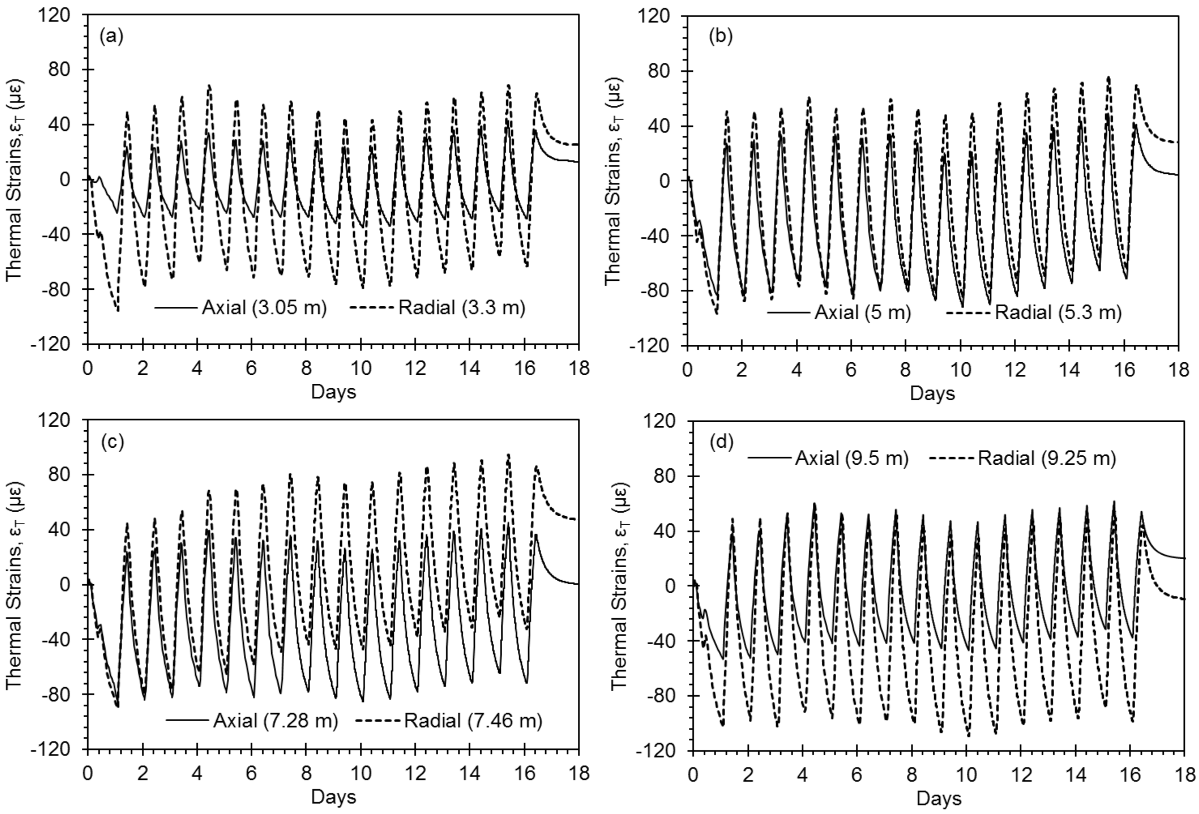

Figure 5. Time series of axial and radial thermal strains at different depths, *d*: a) d ≈ 3 m b) d ≈ 5 m c) d ≈ 7 m d) d ≈ 9 m.

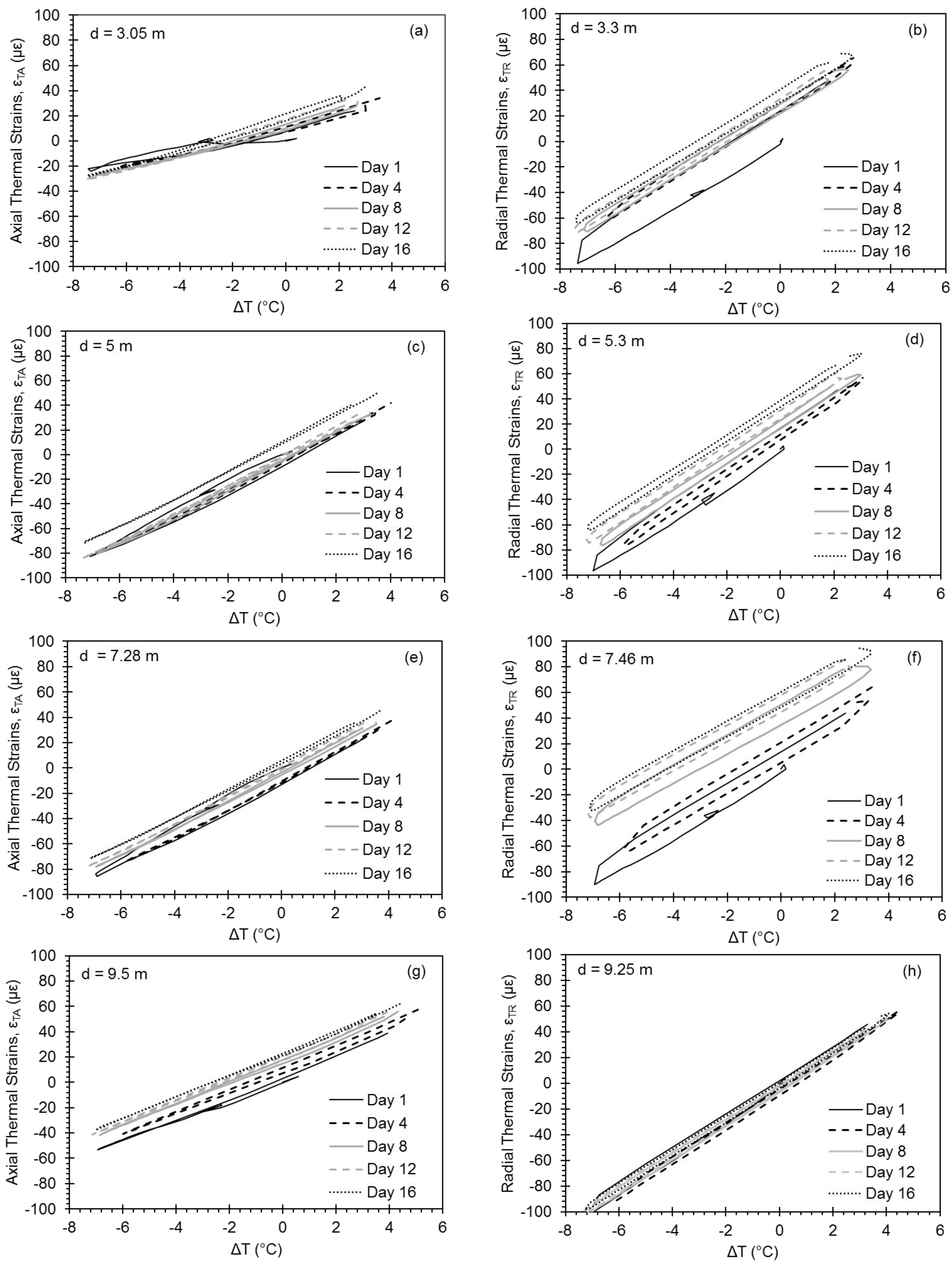

Figure 6. Axial (ε_{TA}) and radial (ε_{TR}) thermal strains plotted against, ΔT, at different depths, *d*: a) ε_{TA} at d = 3.05 m b) ε_{TR} at d = 3.3 m c) ε_{TA} at d = 5

m d) ε_{TR} at d = 5.3 m e) ε_{TA} at d = 7.28 m f) ε_{TR} at d = 7.46 m g) ε_{TA} at d = 9.5 m h) ε_{TR} at d = 9.25 m.

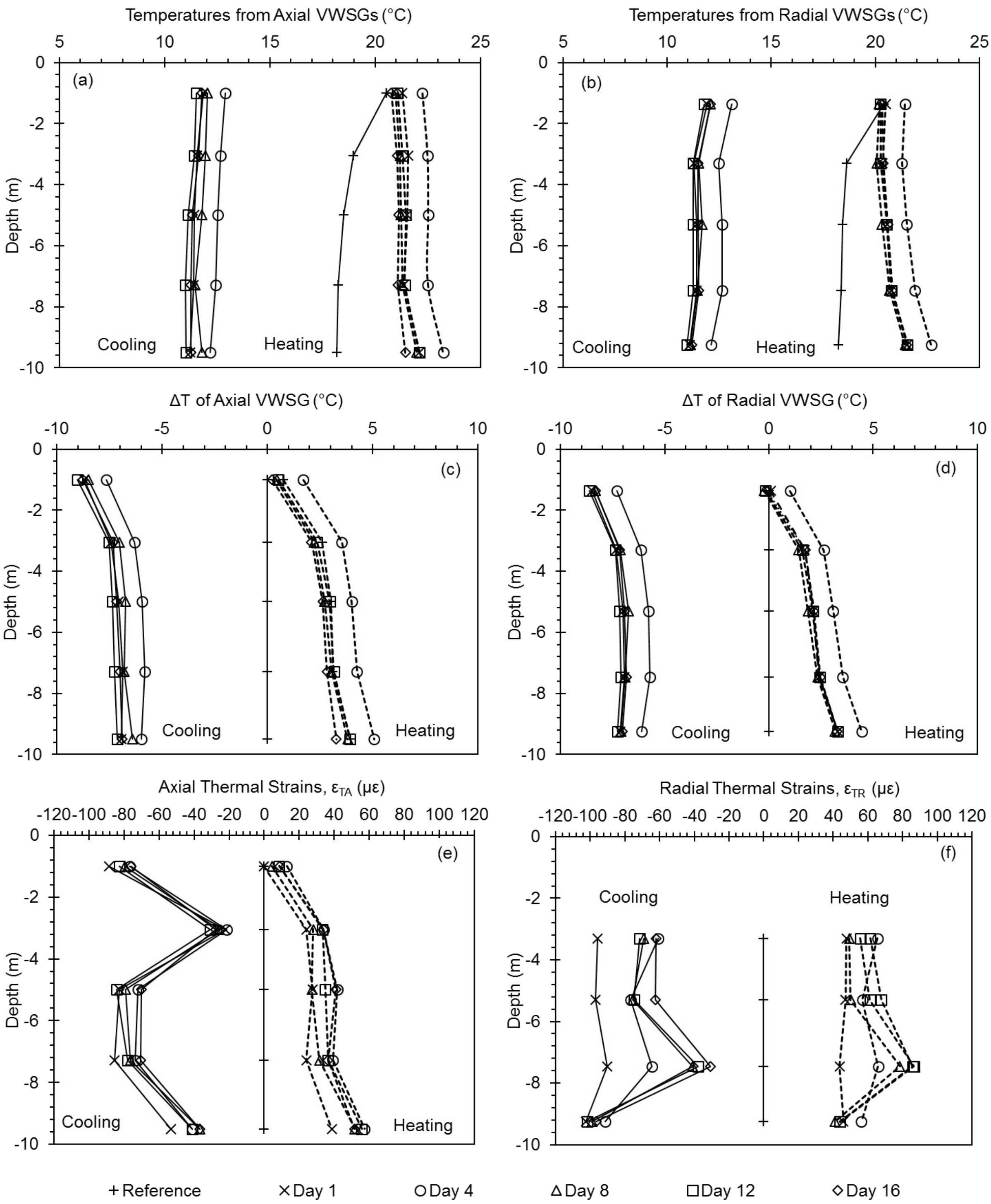

Figure 7. Pile temperatures and thermal strains plotted against depth (dashed line – end of heating; solid line – end of cooling): pile

temperatures from axial VWSGs b) pile temperatures from radial VWSGs c) change in pile temperatures, ΔT, from axial VWSGs d) change in pile temperatures ΔT, from radial VWSGs e) axial thermal strains f) radial thermal strains.

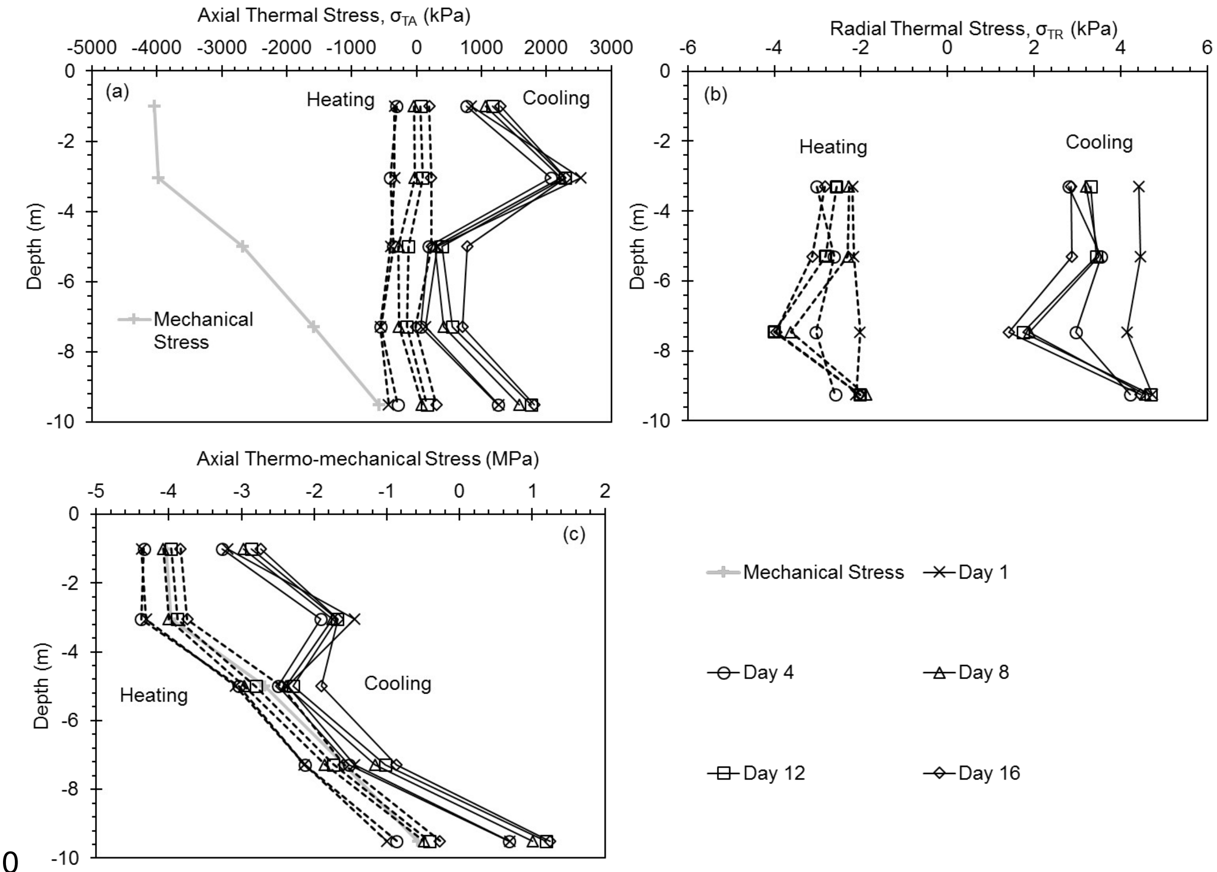

Figure 8. Thermal and thermo-mechanical loads (dashed line – end of heating; solid line – end of cooling): a) axial thermal stresses b) radial thermal stresses c) axial thermo-mechanical stresses.

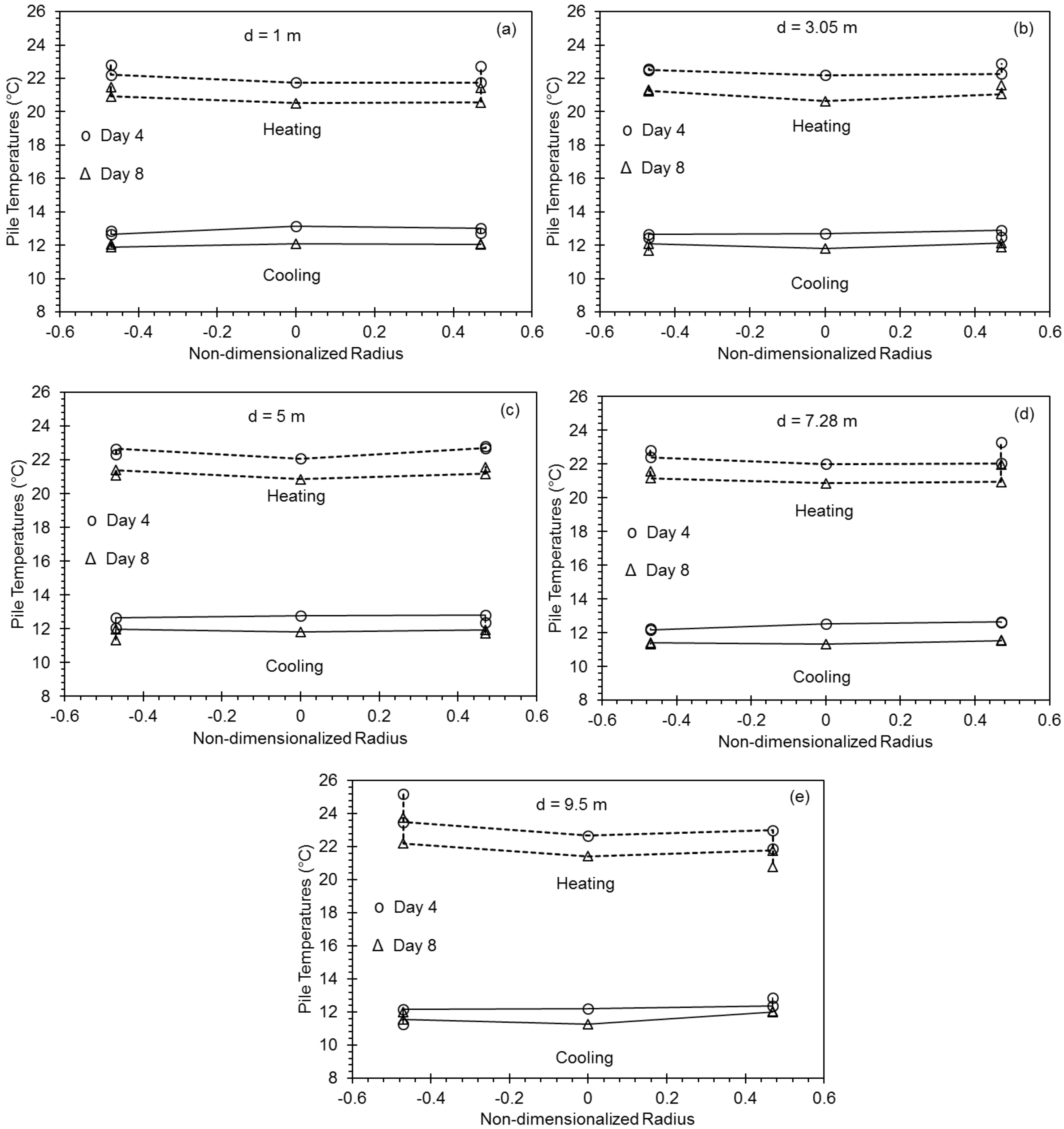

Figure 9. Temperature distribution over the planar cross-section of the energy pile at different depths, *d* (dashed line – end of heating; solid line – end of cooling): a) d = 1 m b) d = 3.05 m c) d = 5 m d) d = 7.28 m e) d = 9.5 m.

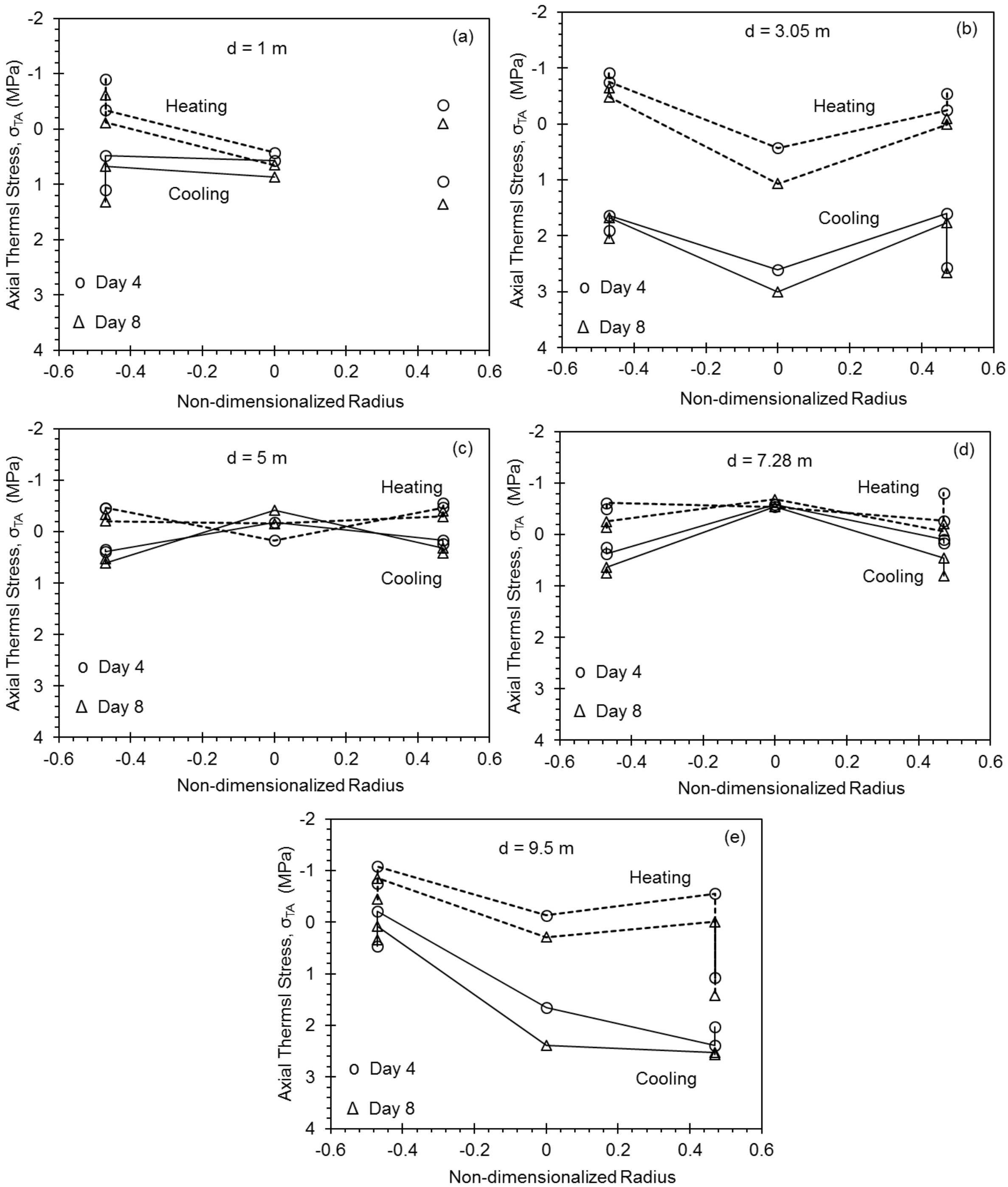

Figure 10. Axial thermal stress distribution over the planar cross-section of the energy pile at different depths, *d* (dashed line – end of heating; solid line – end of cooling): a) d = 1 m b) d = 3.05 m c) d = 5 m d) d = 7.28 m e) d = 9.5 m.